08.2;01.1

Kinetics of spontaneous formation of core shell structure in (In,Ga)As nanowires

© N.V. Sibirev [1], Y.S. Berdnikov [1–3], I.V. Shtrom [1,4], E.V. Ubyivovk [1,2], R.R. Reznik [1,2], G.E. Cirlin [1,2,4]

[1] St. Petersburg State University, St. Petersburg, Russia
[2] Alferov Federal State Budgetary Institution of Higher Education and Science Saint Petersburg National Research Academic University of the Russian Academy of Sciences, St. Petersburg, Russia
[3] National Research University Higher School of Economics, St. Petersburg, Russia
[4] Institute of Analytical Instrument Making, Russian Academy of Sciences, St. Petersburg, Russia
E-mail: N.Sibirev@spbu.ru

Received May 13, 2021
Revised October 21, 2021
Accepted October 22, 2021

A model of spontaneous formation of the core-shell structure in (In,Ga)As nanowire grown via molecular beam epitaxy without independent radial growth is proposed. Within the framework of the proposed model, the distribution of In across the axis of the nanowire was fitted.

Keywords: core-shell nanowire, ternary nanowire, InGaAs nanowire, radial nanowire heterostructure.

DOI: 10.21883/TPL.2022.02.52841.18869

III–V semiconductor nanowires (NWs) are used as the basic elements for active regions of a whole series of new optoelectronic devices [1–3]. Highly developed lateral surfaces of NW make them well-suited for sensorics applications [2,3] and allow one to combine materials with widely different lattice parameters in a single core–shell structure [3].

Molecular beam epitaxy (MBE) is currently one of the most widely used techniques for III–V NWs growth [2,3]. The cores of core–shell NWs are typically grown using vapor–liquid–solid (VLS) or vapor–solid–solid techniques with a liquid droplet or a solid particle of a catalyst on top. The shell is formed as a result of independent vapor–solid (VS) material deposition on the lateral surfaces of NWs [4]. The nonuniformity of radial growth along the NW axis in such growth processes results in the formation of structures tapering toward the top [4]. In addition, it was demonstrated experimentally that the doping levels in VLS core growth and VS shell growth may differ by an order of magnitude [5].

In the present study, an alternative model of (In,Ga)As core–shell NW formation in a single process without the independent radial growth is introduced. A model characterizing the mechanism of formation of such NWs in the process of MBE growth is proposed for the first time, and simulated data are compared with the experimental ones.

NWs are typically grown layer-by-layer [6], and the composition of each monolayer (ML) is defined by the rates of incorporation of components into the moving step of the ML being formed [7,8]. Various formulae [6–9] are used to characterize this effect. Here, we use the formula from [8]:

$$x = \frac{v_{\mathrm{InAs}}}{v_{\mathrm{InAs}} + v_{\mathrm{GaAs}}}, \qquad (1)$$

where v_{InAs} and v_{GaAs} are the rates of incorporation of In–As and Ga–As atom pairs into the step.

If the critical nucleus of a new ML is assumed to be small-sized [9,10], the rates of incorporation of In–As and Ga–As atom pairs into the step may be characterized using the following formulae [11,12]:

$$v_{\mathrm{InAs}} = k_{\mathrm{InAs}} C_{\mathrm{As}} C_{\mathrm{In}}, \qquad (2)$$

$$v_{\mathrm{GaAs}} = k_{\mathrm{GaAs}} C_{\mathrm{As}} C_{\mathrm{Ga}}. \qquad (3)$$

Here, C_{As}, C_{Ga}, and C_{In} are the concentrations of arsenic, gallium, and indium in the catalyst droplet; k_{InAs} and k_{GaAs} are kinetic coefficients.

Let us introduce the following dimensionless quantities for further analysis: $k = \frac{k_{\mathrm{InAs}}}{k_{\mathrm{InAs}}+k_{\mathrm{GaAs}}}$, $y = \frac{C_{\mathrm{In}}}{C_{\mathrm{Ga}}+C_{\mathrm{In}}} = \frac{N_{\mathrm{In}}}{N_{\mathrm{Ga}}+N_{\mathrm{In}}}$, where N_{In} and N_{Ga} are the numbers of indium and gallium atoms in the catalyst. If we use this notation in Eq. (1), the relation between catalyst composition y and composition x of the moving step is written as

$$x = \frac{ky}{2ky - k - y + 1}. \qquad (4)$$

In MBE growth of (In,Ga)As NWs, number N of group III atoms in the catalyst is defined by the overall fluxes of In (F_{In}) and Ga (F_{Ga}) atoms and the rate of incorporation of atoms into the step of a new ML. To make the form of equations more convenient, we express the numbers of atoms in a droplet N, N_0, N_{In}, and N_{Ga} in an ML. The movement rate of the step is limited by the influx of As from a gas medium (the flux of arsenic is denoted as F_{As}), since the solubility of As in a catalyst droplet is lower than the corresponding parameter of In and Ga [1,13]. Introducing notation $f = \frac{F_{\mathrm{As}}}{F_{\mathrm{In}}+F_{\mathrm{Ga}}}$, $z = \frac{F_{\mathrm{In}}}{F_{\mathrm{Ga}}+F_{\mathrm{In}}}$, we obtain the following

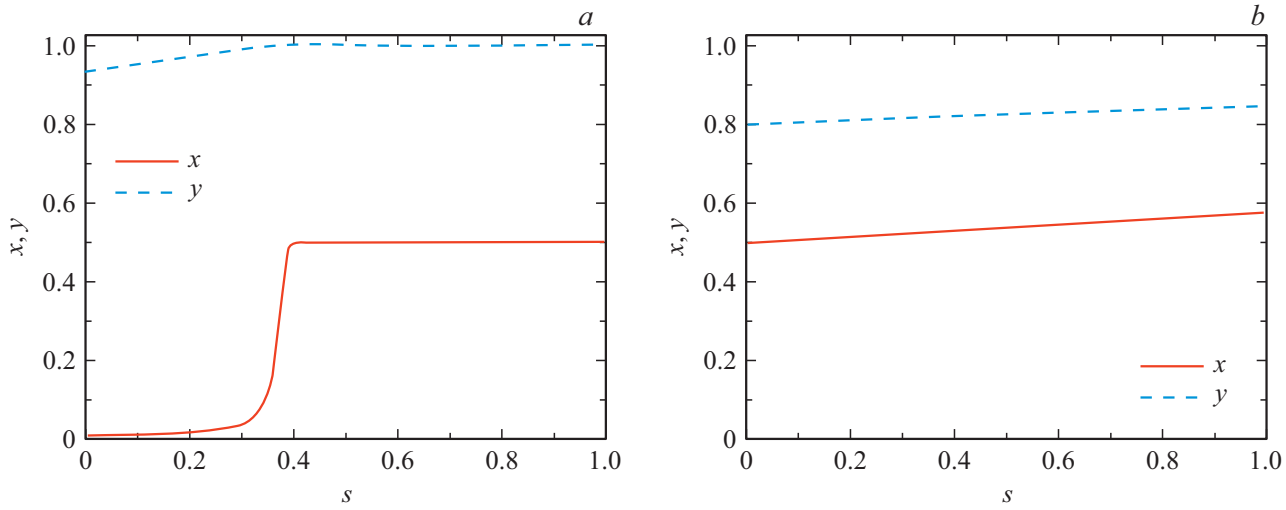

Figure 1. Variation of the step composition (x) and the droplet composition (y) in the process of monolayer filling (s). a — parameters $k = 0.00045$, $N_0 = 3$, $z = 0.3$, $f = 1.4$, $y_0 = 0.94$; b — parameters $k = 0.2$, $N_0 = 3$, $z = 0.5$, $f = 2$, $y_0 = 0.8$.

equation for N:

$$\frac{dN}{ds} = \frac{1}{f} - 1, \tag{5}$$

where $s = F_{\mathrm{As}}t$ is the filling of the top face of an NWs that varies from 0 to 1. The equation for the amount of indium in a droplet then takes the form

$$\frac{d(yN)}{ds} = \frac{z}{f} - x. \tag{6}$$

Let us denote the number of group III atoms in the catalyst at the moment of nucleation of a new ML $(s = 0)$ as N_0. Equation (6) with (4) taken into account may then be written as

$$\frac{(1-2k)y - 1 + k}{\left((1-2k)y - 1 + k\right)\left(y + \frac{z}{f-1}\right) + \frac{fk}{f-1}y}\frac{dy}{ds} = \frac{1}{\frac{f}{f-1}N_0 - s}. \tag{7}$$

Taken together with initial condition $y(0) = y_0$, Eqs. (4) and (7) characterize the dynamics of variation of the droplet composition and the composition of the ML being formed.

Typical examples of dependences of the compositions of the catalyst and the growing ML are presented in Fig. 1. Fig. 1, a illustrates the case when the concentration of a rapidly crystallizing element (Ga) in the droplet decreases exponentially in the process of ML growth. When this occurs, the rate of incorporation of In into the NWs at the initial stage of ML formation is almost zero (i.e., $x \approx 0$). The fraction of a highly soluble element (In) in the droplet grows in the process of ML formation and eventually becomes almost equal to unity (i.e., $y \sim 1$). At the next (end) stage of ML formation, its composition is defined by the influx of a rapidly crystallizing element (Ga), and $x \approx 1 - \frac{1-z}{f}$. The case with a poorly soluble and rapidly crystallizing element (Ga) remaining unconsumed within the time period of ML formation is presented in Fig. 1, b for comparison.

In order to calculate the composition profile in the transverse NW section, one needs to determine the shape of the nucleus and the site where it forms. The data of *in situ* observations of the growth of individual MLs in NWs, we suggest that the nucleus of a new layer forms at the vertex of the top NW face and is triangular in shape [9,10] (see in the inset in Fig. 2, a). Since the probabilities of formation of the nucleus in each of the six vertices of the top face are equal, one needs to perform averaging over six corners to obtain the NW composition profile.

With this geometry of the nucleus, the ML filling after averaging over all six NWs vertices is the same at all points within the hexagon and is equal to $1/2$. Therefore, linear dependence $x(s)$ of the step composition on filling (see the example in Fig. 1, b) should result in a uniform composition in the transverse NW section.

A highly nonlinear dependence of the step composition on filling (see the example in Fig. 1, a) is needed to produce an NW that is nonuniform in the transverse section. Fig. 2, a presents an example nonuniform distribution of In in the transverse NW section. The concentration of In at the(In,Ga)As NW center (in the core) is higher than that at the periphery (in the shell). Thus, depletion of the catalyst droplet in Ga may result in the formation of a core−shell structure in the process of VLS growth. More generally, the shell may be enriched either with Ga, which is poorly soluble in the droplet, or with highly soluble In depending on the growth parameters.

The parameter values corresponding to the conditions of MBE (In,Ga)As NW growth experiments were used to calculate the NWs composition profile in Fig. 2, a. The growth of NWs with a gold catalyst was performed on Si(111) substrates within 20 min under As-stabilized

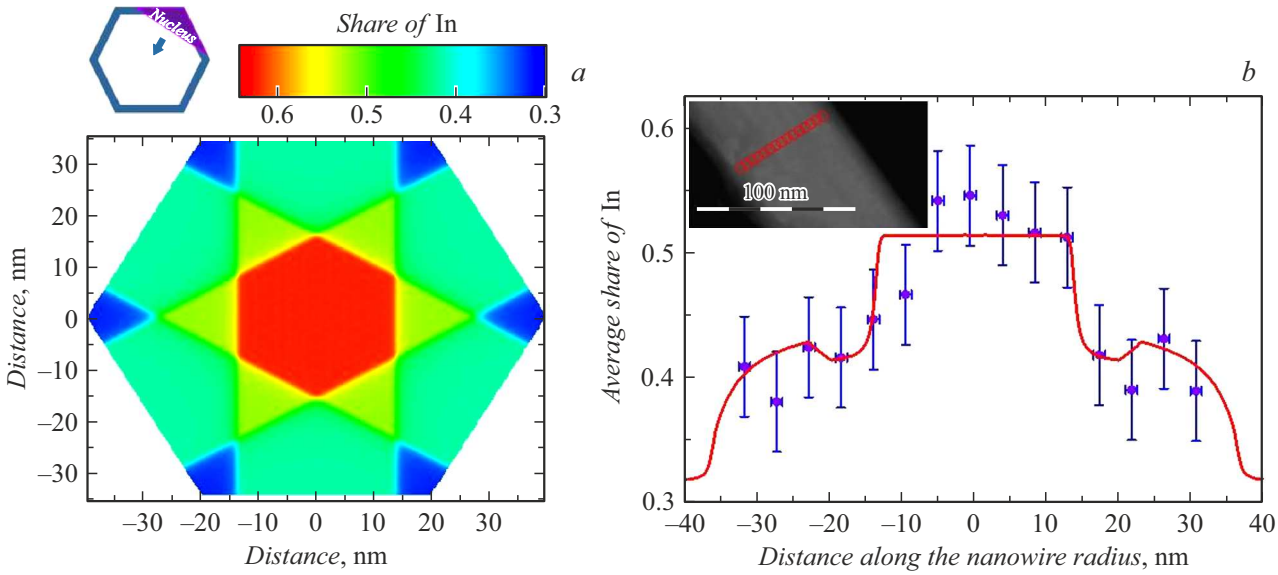

Figure 2. *a* — calculated composition profile in the transverse section of an NW; *b* — composition profile transverse to the NWs axis. Dots — represent experimental data, while the solid curve corresponds to the results of calculations with parameters $z = 0.46$, $N_0 = 2.4$, $f = 1.42$, $k = 5.4 \cdot 10^{-4}$, and $y_0 = 0.96$.

conditions. Therefore, the ratio of fluxes of groups V/III for simulations was set within the $f = 1-1.5$ range. The effective deposition rate and the growth temperature were kept constant and equal to 0.8 ML/s and 220°C.

The composition profile transverse to the NW axis was measured with a Zeiss Libra 200FE transmission electron microscope (TEM) fitted with an Oxford X-Max 80 energy dispersive X-ray (EDX) detector. An example TEM image of an NW and the results of measurement of the composition transverse to the NWs axis are presented in Fig. 2, *b*. The enrichment of the central NW part with indium is observed experimentally. The fraction of In is approximately 50% in the inner third of the NW and approximately 40% at the periphery. The enrichment of the shell with Ga may be attributed to its more active (compared to In) incorporation at the initial stage of ML formation.

It is known that the concentration of Ga in the droplet in the process of autocatalytic growth of (In,Ga)As NW remains at the detection limit of EDX detectors (below 5%) even when the fraction of Ga in NWs becomes as high as 80–90% [14]. Therefore, $k < 0.002$.

Following the termination of growth, gold droplets with radii smaller than 5 nm were observed at the apices of NWs. This allows one to estimate the gold concentration in the droplet during growth. The droplet diameter in the process of growth is approximately equal to the NW diameter (i.e., is larger than 50 nm). If the droplet height remained constant during growth, the gold concentration may be estimated as the ratio of the solidified droplet diameter squared and the NW diameter squared (i.e., below 1% in the present case). Therefore, the droplet consists almost exclusively of In and Ga with their melting points below the growth temperature.

More accurate parameter values were obtained by approximating the results of measurements of the composition transverse to the NWs axis (Fig. 2, *b*) with a model dependence. The calculated In distribution within the transverse NW section (Fig. 2, *a*) was averaged for this purpose along the axis perpendicular to the scan direction. Parameter $z = 0.46$ was determined as the average NW composition. The values of model parameters were then fitted by gradient descent. The best fit between the calculated dependence and the experimental one was obtained at $k = 0.00054$, $N_0 = 2.4$, $f = 1.42$, and $y_0 = 0.96$. The fraction of Ga in the droplet reaches its maximum (approximately 4%) at the moment of ML nucleation, but decreases rapidly to less than 0.1% in the process of ML growth and remains at this level till the completion of this ML.

We note in conclusion that a model characterizing the spontaneous formation of a radial core–shell structure in (In,Ga)As NW was proposed in the present study. The calculated NW composition profiles agree well with the experimental data obtained in the process of MBE NWs growth.

Funding

The growth of NW and simulations were supported financially by the Russian Science Foundation (project No. 18-72-10047). NWs diagnostics were performed using the equipment of the Interdisciplinary Resource Center for Nanotechnology (St. Petersburg State University) and were supported by grant No. 75746688 from St. Petersburg State University. R.R. Reznik acknowledges support from the Ministry of Science and Higher Education of the Russian Federation, research project No. 2019-1442. Yu.S. Berd-

nikov acknowledges support from the National Research University Higher School of Economics granted as part of its Fundamental Research Program for 2021.

Conflict of interest

The authors declare that they have no conflict of interest.

References

[1] V.G. Dubrovskii, G.E. Cirlin, V.M. Ustinov, Semiconductors, **43** (12), 1539 (2009). DOI: 10.1134/S106378260912001X.
[2] E. Barrigón, M. Heurlin, Z. Bi, B. Monemar, L. Samuelson, Chem. Rev., **119**, 9170 (2019). DOI: 10.1021/acs.chemrev.9b00075
[3] M. Royo, M. De Luca, R. Rurali, I. Zardo, J. Phys. D: Appl. Phys., **50**, 143001 (2017). DOI: 10.1088/1361-6463/aa5d8e
[4] V.G. Dubrovskii, I.V. Shtrom, R.R. Reznik, Y.B. Samsonenko, A.I. Khrebtov, I.P. Soshnikov, S. Rouvimov, N. Akopian, T. Kasama, G.E. Cirlin, Cryst. Growth Des., **16**, 7251 (2016). DOI: 10.1021/acs.cgd.6b01412
[5] E. Dimakis, M. Ramsteiner, A. Tahraoui, H. Riechert, L. Geelhaar, Nano Res., **5**, 796 (2012). DOI: 10.1007/s12274-012-0263-9
[6] V.G. Dubrovskii, N.V. Sibirev, G.E. Cirlin, Tech. Phys. Lett., **30** (8), 682 (2004). DOI: 10.1134/1.1792313.
[7] P. Periwal, N.V. Sibirev, G. Patriarche, B. Salem, F. Bassani, V.G. Dubrovskii, T. Baron, Nano Lett., **14**, 5140 (2014). DOI: 10.1021/nl5019707
[8] J. Johansson, M. Ghasemi, Phys. Rev. Mater., **1**, 040401 (2017). DOI: 10.1103/PhysRevMaterials.1.040401
[9] C.B. Maliakkal, E.K. Mårtensson, M.U. Tornberg, D. Jacobsson, A.R. Persson, J. Johansson, L.R. Wallenberg, K.A. Dick, ACS Nano., **14**, 3868 (2020). DOI: 10.1021/acsnano.9b09816
[10] J.C. Harmand, G. Patriarche, F. Glas, F. Panciera, I. Florea, J.-L. Maurice, L. Travers, Y. Ollivier, Phys. Rev. Lett. **121**, 166101 (2018). DOI: 10.1103/PhysRevLett.121.166101
[11] N.V. Sibirev, Tech. Phys. Lett., **41** (3), 209 (2015). DOI: 10.1134/S1063785015030153.
[12] V.G. Dubrovskii, Tech. Phys. Lett., **42** (3), 332 (2016). DOI: 10.1134/S1063785016030196.
[13] P. Krogstrup, H.I. Jørgensen, E. Johnson, M.H. Madsen, C.B. Sørensen, A.F.I. Morral, M. Aagesen, J. Nygård, F. Glas, J. Phys. D: Appl. Phys., **46** (31), 313001 (2013). DOI: 10.1088/0022-3727/46/31/313001
[14] A. Scaccabarozzi, A. Cattoni, G. Patriarche, L. Travers, S. Collin, J.C. Harmand, F. Glas, F. Oehler, Nanoscale, **12**, 18240 (2020). DOI: 10.1039/d0nr04139d